$$I_n=2eE_x n_B\mu_n\lambda_n \times\left(\int_{u_B-u_S}^{0} d\nu\, e^{-\nu}[e^{2K_n(v_{zS},0)}-2K_n(v_{zS},0)-1] +\int_0^{\infty} d\nu\, e^{-\nu}[e^{-K_n(v_{zB},v_{zS})}+2K_n(v_{zB},v_{zS})-1]\right). \quad (A.1)$$

But

$$K_n(v_{zB},v_{zS})=-\int_{v_{zB}}^{v_{zS}}\frac{m dv_z}{e\tau E_z}=\int_0^d dz/\tau v_z \quad (A.2)$$

$$=\frac{d}{\tau v_{zB}}-\int_0^d\frac{dz}{\tau}\left(\frac{v_z-v_{zB}}{v_z v_{zB}}\right). \quad (A.3)$$

Thus, for $d\gg\lambda_n$, the first term of the second integral in (A.1) vanishes, and, noting that $\nu=mv_{zB}^2/2kT$, (A.1) becomes

$$I_n=2eE_x n_B\mu_n(d-\lambda_n)+2eE_x\Delta N\mu_n\frac{n_B\lambda_n}{\Delta N} \times\left\{\int_{u_B-u_S}^{0} d\nu\, e^{-\nu}[e^{2K_n}-2K_n-1] +2\int_0^{\infty} d\nu\, e^{-\nu}\int_0^d\frac{dz}{\tau}\left(\frac{v_{zB}-v_z}{v_z v_{zB}}\right)\right\}, \quad (A.4)$$

from which (4.4) follows.

ACKNOWLEDGMENTS

It is a pleasure to thank W. H. Brattain, C. G. B. Garrett, and B. Levinger for helpful discussions and A. Brown and E. Thomas for the numerical computations.

PHYSICAL REVIEW VOLUME 118, NUMBER 4 MAY 15, 1960

Zeeman Effect of Impurity Levels in Silicon*

SOLOMON ZWERDLING, KENNETH J. BUTTON, AND BENJAMIN LAX
Lincoln Laboratory, Massachusetts Institute of Technology, Lexington, Massachusetts

(Received December 28, 1959)

Completely resolved Zeeman spectra for the bismuth donor in silicon including optical transitions from the $1s$ donor ground state to the excited states $2p_0$, $2p_\pm$, $3p_0$, $4p_0$, $3p_\pm$, $5p_0$, $4p_\pm$, and $5p_\pm$ are presented. The transitions were observed at liquid helium temperature, using linearly polarized radiation alternately parallel and perpendicular to the magnetic field, and field intensities up to 38.9 kilogauss oriented along each of the three principal crystallographic axes. Both linear splitting of the $p_\pm$ states and a quadratic dependence on field were observed. The use of impurity Zeeman spectra is demonstrated for evaluating effective mass parameters, determining the nature of energy bands and finding and identifying impurity excited states. The transverse effective mass for the electron in silicon was found to be $(0.186\pm0.006)\ m_0$ in agreement with recent cyclotron resonance results. From Zeeman splitting, electron effective masses up to $0.5\ m_0$ can be measured to within $\pm\frac{1}{2}\%$ at infrared frequencies in a field of 40 kilogauss. The behavior in a magnetic field of the first two donor excited states could be explained by treating the magnetic terms of the Hamiltonian as a perturbation to first order. Interactions among the higher closely-spaced Zeeman levels were observed above 20 kilogauss and were evaluated with a second-order treatment. The Zeeman structure for the aluminum acceptor reflected the complexity of the valence bands and the acceptor ground state and was in qualitative agreement with the theoretical results of Kohn and Schechter. Transitions were observed to eight excited states converging to the series limit. Evidence is given for the degeneracy of each state.

I. INTRODUCTION

IT has been realized that measurement of the Zeeman effect of the excited states of the monovalent donor and acceptor impurities in semiconductors offers a means of studying the energy band structure and the effective masses of carriers. Theoretical evaluation[1–3] of the linear Zeeman effect for donors in Ge and Si had indicated that the Zeeman splitting should be resolvable by spectroscopic techniques. For germanium, a linear splitting for the transition $1s\rightarrow 2p_\pm(m=\pm1)$ for both As and P impurities was reported by Fan and Fisher,[4] and similar measurements in the far infrared region were also reported by Boyle[5] for As impurity. Transitions from the ground state to quantized magnetic levels in the conduction band were also observed and the effective mass of the electron was determined. For silicon, both linear and quadratic Zeeman effects were observed for the bismuth donor[3] and a preliminary Zeeman spectrum for Si(Bi) was presented by Zwerd-

* The work reported in this paper was performed by Lincoln Laboratory, a center for research operated by Massachusetts Institute of Technology with the joint support of the U. S. Army, Navy, and Air Force.

[1] B. Lax, R. D. Puff, and W. H. Kleiner, Bull. Am. Phys. Soc. 3, 31 (1958).
[2] R. R. Haering, Can. J. Phys. 8, 1161 (1958).
[3] B. Lax, L. M. Roth, and S. Zwerdling, J. Phys. Chem. Solids 8, 311 (1959).
[4] H. Y. Fan and P. Fisher, J. Phys. Chem. Solids 8, 270 (1959).
[5] W. S. Boyle, J. Phys. Chem. Solids 8, 321 (1959).

ling, Button, and Lax.[6] More extensive theoretical work has been reported[7] which involves both the linear and quadratic Zeeman effects and takes into account the interaction between higher excited states in the presence of a magnetic field.

The theory of the Zeeman effect for the ground state of acceptors has been treated by Kohn.[8] For the higher excited states of acceptors the theory is much more complicated, and although it has been formulated,[9] the results are not yet available. The experimental data of Fisher and Fan[10] for acceptors in Ge show twofold splitting of the $1s \rightarrow 2p^{(2)}$ and $1s \rightarrow 2p^{(3)}$ transitions with a quadratic shift in the latter.[11]

The purpose of this paper is to present a complete Zeeman spectrum for the bismuth donor in silicon including all of the excited states up to $5p_{\pm}$ and also for the aluminum acceptor including all of the excited states previously observed at zero magnetic field.[12] The anisotropy of these levels will also be reported for both impurities. Magnetic field intensities up to 38.9 kgauss and linearly polarized radiation were used. The donor spectrum was completely resolved and both the linear and quadratic field-dependence of the excited states were determined. The effects of the interaction between adjacent states in the presence of a magnetic field were also observed and evaluated. In the acceptor spectrum, the 38.9 kgauss field was not sufficiently large to resolve the structure in all levels but indications of twofold and fourfold splitting were detected and the quadratic dependence on field was evident for the highest excited states.

The Zeeman spectra for the donor excited states obtained from these experiments permitted the identification of the transitions from the ground state to the various excited states by comparing the behavior of the levels in a magnetic field with a first-order theory. Furthermore, the transverse effective mass of the electron determined from the linear Zeeman splitting was in excellent agreement with the microwave cyclotron resonance result. The degeneracies and relative energies found for the acceptor excited states were consistent with the zero-field theory of Kohn[11] and Schechter.[13]

II. THE PHYSICAL PHENOMENON

The theory of the linear and quadratic Zeeman effects of impurity levels in a semiconductor can be illustrated by considering the theory for a charge carrier having a spherical energy surface. The Schrödinger equation has the familiar form

$$\left(-\frac{\hbar^2}{2m^*}\nabla^2-\frac{\hbar\omega_c}{2i}\frac{\partial}{\partial\phi}+\frac{m^*\omega_c^2}{8}r^2\sin^2\theta-\frac{e^2}{\kappa r}\right)\psi=\mathcal{E}\psi \quad (1)$$

where m^* is the effective mass of the carrier, $\omega_c=eB/m^*c$ is the cyclotron frequency (Gaussian units) in the magnetic field B, and κ is the infrared dielectric constant of the host crystal. The first term on the left of Eq. (1) is the usual momentum term. The second term, which is linear in the magnetic field, is responsible for the ordinary linear Zeeman splitting. The third term is associated with the diamagnetic, or quadratic, Zeeman effect. The circumstances of interest are those for which the terms involving the magnetic field can be treated as a perturbation. It is then permissible to use the zero-field wave functions to evaluate the change in the eigenvalue due to the magnetic field. The zero field wave functions for p states are proportional to $e^{im\phi}$ where m is the azimuthal quantum number of the angular momentum. Applying the second term of Eq. (1) to ψ yields the energy shift for each p state

$$\Delta\mathcal{E}_m=m\hbar\omega_c/2 \quad (2)$$

which is linear in the magnetic field and nonvanishing only for $m=\pm1$. Since the transitions at low temperature are those from the $1s$ ground state to these p-states, then a linear splitting can occur only for $\Delta m=\pm1$. The degeneracy of the $p_{\pm}$ states is removed by the magnetic field, and the states are split by the magnitude $\Delta\mathcal{E}_{\pm}=\hbar\omega_c$. Therefore, the effective mass of an isotropic carrier can be measured directly from the linear Zeeman effect. However, in order to observe the transitions involving $\Delta m=\pm1$ spectrometrically, it is necessary that the electric vector of the radiation have a component along the oscillating electric dipole moment associated with the $p_{\pm}$ states. Since, for the latter, the dipole moment oscillates at right angles to the magnetic field, then the transitions will occur in plane polarized radiation only for $\mathbf{E}\perp\mathbf{B}$, where $\mathbf{E}$ is the electric vector of the incident radiation and $\mathbf{B}$ is the dc magnetic field. Similar reasoning indicates that for $\mathbf{E}\|\mathbf{B}$, transitions are induced only to the p_0 states for which $\Delta m=0$, and there is no linear dependence on field as shown by Eq. (2). Measurements with polarized radiation would thus improve experimental resolution since the polarized spectra are mutually exclusive and overlapping of lines is greatly reduced.

At higher fields, the quadratic term becomes effective. It can be shown[14] that, for $\ell=1$, $m=0$ (p_0 states)

$$\Delta\mathcal{E}=\frac{\kappa^2\hbar^4\omega_c^2}{e^4m^*}\frac{n^2}{8}(n^2-1). \quad (3)$$

[6] S. Zwerdling, K. J. Button, and B. Lax, Bull. Am. Phys. Soc. 4, 145 (1959).

[7] W. H. Kleiner, R. N. Brown, and B. Lax, Bull. Am. Phys. Soc. 4, 144 (1959).

[8] W. Kohn (private communication).

[9] W. H. Kleiner (private communication).

[10] P. Fisher and H. Y. Fan, Phys. Rev. Letters 2, 456 (1959).

[11] This notation is that of W. Kohn, *Solid State Physics*, edited by F. Seitz and D. Turnbull (Academic Press, Inc., New York, 1957), Vol. 5, p. 303, Table VII.

[12] H. J. Hrostowski and R. H. Kaiser, J. Phys. Chem. Solids 4, 148 (1958).

[13] D. Schechter, "Theory of shallow acceptor states in Si and Ge," doctoral thesis, Department of Physics, Carnegie Institute of Technology, Pittsburgh, Pennsylvania, 1958.

[14] See, for example, J. H. Van Vleck, *The Theory of Electric and Magnetic Susceptibilities* (Oxford University Press, London, 1932), p. 178.

Therefore, the quadratic Zeeman effect varies inversely as the cube of the effective mass and directly as the square of the dielectric constant for different host materials. The quadratic shift with field also becomes increasingly more important for the higher excited states for which it varies as n^4.

The above analysis can be applied only qualitatively to silicon because the band structure is more complicated for both donors and acceptors. The conduction band consists of six minima along the $\langle 100\rangle$ axes and the constant energy surfaces in momentum space are represented by ellipsoids of revolution about these axes. The theory of the donor states has been considered previously at zero field.[15] The Hamiltonian, including magnetic terms, can be written in the form

$$\mathcal{H}=\frac{\pi_x^2+\pi_y^2}{m_t}+\frac{\pi_z^2}{m_l}+V \tag{4}$$

where

$$\pi_j=\frac{\hbar}{i}\frac{\partial}{\partial j}-\frac{eA_j}{c},$$

$\mathbf{A}=\frac{1}{2}\mathbf{r}\times\mathbf{B}$ is the magnetic vector potential, $V=-e^2/\kappa r$ is the Coulomb potential energy and m_t and m_l are the transverse and longitudinal effective masses. Equation (4) can be expanded to give a Hamiltonian containing linear and quadratic terms in the magnetic field. Again, treating the magnetic terms as a perturbation, the zero-field solution and wave functions can be used to calculate both the linear and quadratic Zeeman effects. The linear problem has been considered by Lax, Puff, and Kleiner,[1] and independently by Haering.[2] They have shown that the linear Zeeman splitting of the $p_\pm$ states is given by

$$\Delta\mathcal{E}_\pm=\hbar\omega_t\cos\theta \tag{5}$$

for each ellipsoid, where $\omega_t=eB/m_tc$ and θ is the angle between the direction of the magnetic field and the major axis of the ellipsoid. The quadratic Zeeman effect of the ground state[1,3] gives a result which is analogous to Eq. (3), and is very small in silicon. At higher fields and for higher excited states where the quadratic effect becomes important, the theoretical problem is not as simple. The perturbation theory has to be carried out to higher order terms and the interaction and coupling between neighboring states in a magnetic field must be taken into account. This problem has been treated by Brown, Kleiner, and Lax.[16]

Equation (5) shows that the linear Zeeman effect depends only on the transverse effective mass; hence at low fields, it is possible to measure m_t from the splitting of the $p_\pm$ states. At higher fields where the quadratic effect is important, both the transverse and longitudinal effective masses enter into the analysis. The anisotropy of the Zeeman spectrum therefore reflects that of the energy bands. However, since the theory is rather complicated, a simple interpretation in terms of these parameters cannot be made.

In the region where the Zeeman effect is linear, it is relatively simple to deduce the selection rules and line intensities for linearly polarized radiation used in these experiments. It can be shown that the transition intensity is proportional to the square of the matrix element $M^2\sim|\langle j|\,\mathbf{E}\cdot\mathbf{p}\,|s\rangle|^2$ where s refers to the ground state and j to one of the excited states. Consequently, the intensity of the absorption has the form:

$$\begin{aligned} &p_\pm \text{ states:}\quad A\sin^2\phi \\ &p_0 \text{ states:}\quad B\cos^2\phi \end{aligned} \tag{6}$$

where $A\sim|\langle j|p_{x,y}|s\rangle|^2$, $B\sim|\langle j|p_z|s\rangle|^2$ and ϕ is the angle that the electric vector $\mathbf{E}$ of the incident radiation makes with the principal axis of the ellipsoid. The coefficient A is finite for the $p_\pm$ states and vanishes for the p_0 states while B is finite for the p_0 states and vanishes for the $p_\pm$ states. These selection rules form the basis for the interpretation of the polarized spectra which will be presented.

The theory of the Zeeman effect of the acceptor states is much more complicated. The theory of the ground state has been considered by Kohn.[8] The zero-field problem has been studied in detail by Schechter[13] who indicates the existence of a complex spectrum in which the ground-state wave functions are linear combinations of s-like and d-like states and, similarly, the excited states involve combinations of p and f functions. The latter appear to have fourfold degeneracy in the first two excited states and twofold degeneracy for the next two higher states. This implies that the ground state should also contribute to the Zeeman spectrum because of the presence of the d states. This has not been observed for silicon because the acceptor ground state is relatively deep, that is, the Coulomb field for it is strong, so that the effect of the magnetic field on the ground state can be neglected. Starting with Schechter's wave functions, it is possible in principle, to work out the Zeeman pattern of the acceptor in Si. Initially, one need consider only the 4×4 matrix associated with the fourfold degenerate $p_{3/2}$ bands. The method in terms of spin Hamiltonians is being treated by Kleiner and until such results are available, the detailed interpretation of the Zeeman spectrum of acceptor states in silicon must be postponed.

III. EXPERIMENTAL TECHNIQUES

The Zeeman spectra of impurity levels were observed by using the low-temperature magnetospectrometric

[15] W. Kohn, *Solid State Physics*, edited by F. Seitz and D. Turnbull (Academic Press, Inc., New York, 1957), Vol. 5, p. 257; C. Kittel and A. H. Mitchell, Phys. Rev. **96**, 1488 (1954); J. M. Luttinger and W. Kohn, Phys. Rev. **97**, 1722 (1955); W. Kohn and J. M. Luttinger, Phys. Rev. **98**, 915 (1955).

[16] R. N. Brown, W. H. Kleiner, and B. Lax (to be published).

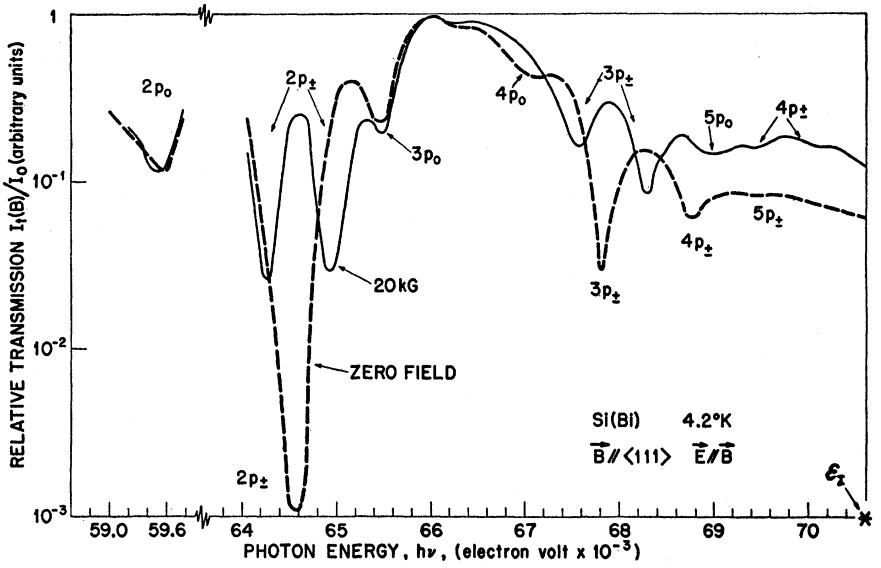

FIG. 1. Photoexcitation spectrum of the bismuth donor in silicon showing transmission minima due to transitions from the bismuth 1s ground state to excited bound states. The linear Zeeman splitting is resolved in a magnetic field of 20 kgauss for the $1s \rightarrow 2p_\pm$, $3p_\pm$, and $4p_\pm$. The quadratic Zeeman effect of the $5p_\pm$ transitions at 20 kgauss has shifted these absorption lines above the zero-field ionization limit denoted by ε_I.

apparatus which has been described previously.[17] The transitions from the ground state to excited states of the bismuth donor and aluminum acceptor in silicon require a photon energy corresponding to the infrared wavelength region between 15 and 23 microns. The measurements were made at 4.2°K using KBr prism double-pass dispersion, and the cryostat containing the doped silicon specimen was equipped with KBr windows. The spectral slit widths achieved ranged from $(1.3\text{–}4.0)\times10^{-4}$ ev and the positions of the transmission minima in the Zeeman spectra were determined to within 2×10^{-5} electron volt for strong lines and 10^{-4} ev for weak lines. Polarized radiation was produced by transmission though a silver chloride sheet pile polarizer set to the Brewster angle. The polarizer could be rotated to align the electric vector of the radiation either parallel or perpendicular to the direction of the dc magnetic field applied to the specimen. Constant magnetic fields were employed and continuous spectra were recorded as a function of wavelength at intervals of five kilogauss up to the maximum of 38.9 kgauss. The specimen was maintained at liquid helium temperature to avoid thermal excitation of the carriers from the impurity ground state.

The silicon samples for these experiments had thicknesses ranging from three to six millimeters, depending upon the impurity concentration and the absorption intensity of the transitions being studied. The optimum concentration range was found to be 10^{15} to 10^{16} impurities/cm^3. Larger concentrations might have caused the overlap of impurity wave functions which would produce loss of spectral detail. Slices were cut from the ingots parallel to a {110} plane and polished flat and parallel. Separate specimens were cut from these slices relative to the three principal crystallographic directions so that the magnetic field would be along one of the crystal axes when the sample was placed in the cryostat. The direction of propagation was therefore normal to the {110} plane and the dc magnetic field was parallel to the {110} plane.

It was found that foreign impurities, particularly oxygen, produced very deleterious effects upon the resolution of the absorption lines. These effects appeared as a severe reduction of absorption intensity and resolution of details, the complete disappearance of absorption maxima, or the introduction of spurious absorptions. In the preparation of bismuth-doped silicon,[18] the added impurity is volatile at the melting temperature of silicon so that it is not convenient to grow the crystal in a vacuum to prevent oxygen contamination. Therefore, it is necessary to add bismuth during the pulling of the crystal in such a way as to minimize the accumulation of foreign impurities that may be present in the bismuth itself. Fortunately, the presence of oxygen in n-type silicon is not as serious as in the p-type material but the data obtained from the seed-end (low oxygen content) showed the best spectral detail. In the case of aluminum-doped silicon,[19] the low vola-

[17] S. Zwerdling, B. Lax, L. M. Roth, and K. J. Button, Phys. Rev. **114**, 80 (1959).

[18] This ingot of Si(Bi) was prepared by Robert L. Hopkins, National Semiconductor Corporation, Danbury, Connecticut. A large donor concentration is required to observe the weak transitions to the highest excited states. High purity and low oxygen content is necessary to permit the resolution of closely spaced lines and to eliminate spurious transitions. A flat resistivity profile makes it possible to prepare similar specimens having different orientations.

[19] We are indebted to Karl Arnold, Sylvania Electric Products Company, Bayside, New York, and Paul Moody, Lincoln Laboratory, Massachusetts Institute of Technology, for this high-purity ingot of Si(Al) having very low oxygen content. This ingot was pulled in a vacuum and the oxygen concentration appeared to be as low as float-zoned material. This is essential if all of the transitions and structure of the Zeeman spectra of aluminum impurity are to be observed.

tility of aluminum permits the crystal to be grown in a vacuum.

IV. EXPERIMENTAL RESULTS AND INTERPRETATION

A. Bismuth Donor

The spectrum of Fig. 1 shows the relative transmission through a three millimeter thick specimen of bismuth-doped silicon as a function of photon energy. The impurity concentration determined from Hall measurements was 5×10^{15} donors/cm^3. The variation in source intensity with wave length as well as atmospheric absorptions were removed in all spectra by taking the ratio of transmission with and without the specimen in the optical path. Lattice absorptions[20] were not removed because transitions to the bismuth excited states occur principally between the medium strength lattice absorption maxima at 0.0637 and 0.0710 electron volt. The plot of the relative transmission on a logarithmic scale results in a spectral curve proportional to the negative of the absorption coefficient, plus a constant, the proportionality factor being the sample thickness. Each transmission minimum of Fig. 1 corresponds to the energy required for an electron transition from the $1s$ ground state to a higher excited donor state. The most striking features of the comparison of the zero-field spectrum with the Zeeman spectrum at 20 kilogauss are the fully-resolved splitting of the $1s\rightarrow 2p_\pm$, $1s\rightarrow 3p_\pm$ and $1s\rightarrow 4p_\pm$ transmission minima. The positions of the levels correspond satisfactorily to the values observed by Hrostowski and Kaiser[21] at zero field with the exception of the very weak $5p_\pm$ level which they did not report. Hrostowski and Kaiser observed the weak

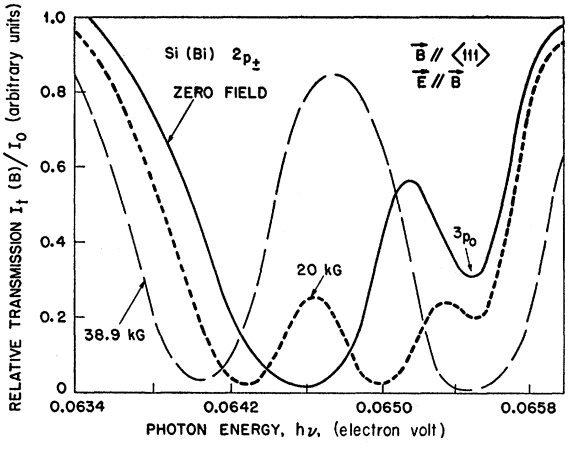

FIG. 2. Zeeman spectrum of the $1s\rightarrow 2p_\pm$ transition at 4.2°K for a specimen three millimeters thick containing 5×10^{16} bismuth donors/cm^3.

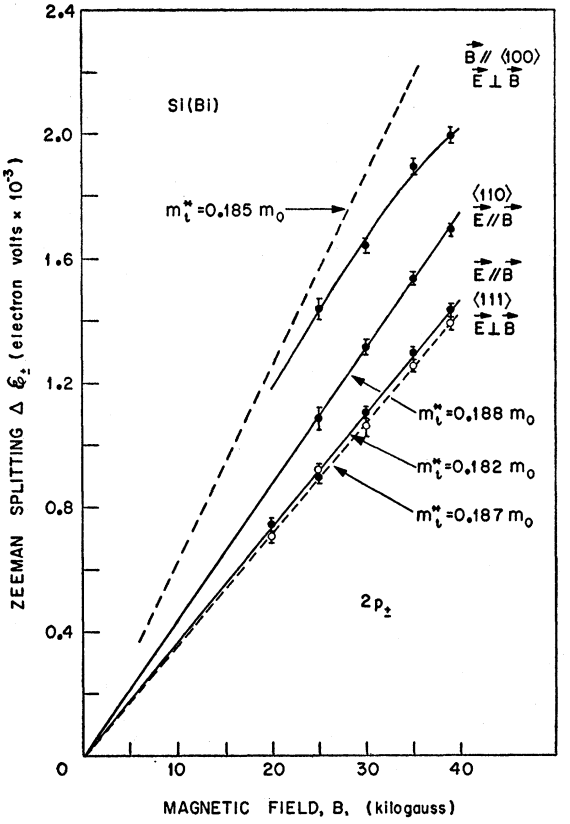

FIG. 3. The linear Zeeman splitting of the $1s\rightarrow 2p_\pm$ transition for several orientations and polarizations. The effective masses were computed from the slope of each line using Eq. (2).

$1s\rightarrow 4p_0$ and $1s\rightarrow 4p_\pm$ transitions but these could not be identified at zero field. The detection and identification of these additional levels was made possible only through the observation of their Zeeman behavior in a magnetic field. For example, the $1s\rightarrow 5p_0$ can be seen at 20 kgauss in Fig. 1 but not at zero field where it has nearly the same energy as the $4p_\pm$.

The Zeeman structure for all transitions is relatively simple for the configuration $\mathbf{B}\|\langle111\rangle$ axis shown in Fig. 1 because all six ellipsoids of the conduction band minimum are equivalent. Figure 2 shows a detailed plot (linear scale) of the Zeeman spectrum of the $1s\rightarrow 2p_\pm$ transition for different values of the magnetic field intensity. The $1s\rightarrow 3p_0$ absorption line is obscured above 25 kgauss by the higher energy component of the $2p_\pm$ level. The splitting of the $1s\rightarrow 2p_\pm$ is given, to first order, by Eq. (5), which can be used to evaluate the transverse effective mass from the observed splitting. This has been plotted in Fig. 3 for the three principal directions and is linear for $\mathbf{B}\|\langle111\rangle$ and $\mathbf{B}\|\langle110\rangle$. However, it is not linear at high fields for $\mathbf{B}\|\langle100\rangle$ indicating interaction between the nearby $3p_0$ and the $2p_\pm$ for this case of largest splitting. The transverse effective mass shown on the figure for each of the linear curves has been determined to an accuracy of $\pm0.001m_0$ due to

[20] R. C. Lord, Phys. Rev. **85**, 140 (1952); R. J. Collins and H. Y. Fan, Phys. Rev. **93**, 674 (1954); M. Lax and E. Burstein, Phys. Rev. **97**, 39 (1955).

[21] H. J. Hrostowski and R. H. Kaiser, J. Phys. Chem. Solids **4**, 315 (1958).

scatter in the data points. Uncertainty in the alignment of the crystal relative to the magnetic field contributes an error of $0.005m_0$ per degree. Therefore we estimate from Eq. (5) and Fig. 3 that $m_t/m_0=0.186\pm0.006$ in agreement with recent cyclotron resonance measurements at 2 millimeter wavelength[22] of $m_t/m_0=0.192\pm0.001$. It is clear that the transverse effective mass could be measured as accurately from Zeeman splitting as from cyclotron resonance if the crystal could be rotated in the field or if linear splitting could be observed for $\cos\theta=1$ [Eq. (5)] where the misalignment error is less serious.

The energy level diagram of Fig. 4 shows the complete Zeeman pattern for $\mathbf{B}\|\langle111\rangle$ and for both alignments of the linear polarization, $\mathbf{E}\perp\mathbf{B}$ and $\mathbf{E}\|\mathbf{B}$. A small quadratic effect appears in the $1s\rightarrow 2p_\pm$ transitions and becomes more pronounced for the higher excited states as expected qualitatively from Eq. (3). The normal order of the hydrogen-like series was observed for the lowest three levels, but the $4p_0$ level appeared at a lower energy than the $3p_\pm$. This inverted order is in accordance with the variational solution of the zero-field theory of excited donor states in silicon.[16] The absorption which we attribute to the $1s\rightarrow 4p_\pm$ transitions showed an initial linear Zeeman splitting of about 3.6×10^{-5} ev/kgauss which is the same as for the $2p_\pm$ and the $3p_\pm$ levels. As the magnetic field was increased, the position of the higher energy component of the $4p_\pm$ approached the maximum of the 0.0710-ev lattice absorption, which greatly reduced the sample transmission and introduced uncertainty in the determination of the position of this weak excited state. It was possible, however, to use unpolarized radiation to obtain the three uppermost curves in Fig. 4 because both polarized spectra are identical for $\mathbf{B}\|\langle111\rangle$. The stronger intensity of unpolarized radiation permitted the use of a thicker specimen (6 mm).

The assignment of the $1s\rightarrow 5p_\pm$ transition was accomplished by comparing the pattern of the observed high field points with the Zeeman pattern calculated[16] from first-order perturbation theory. Transitions to an additional level, designated $5p_0$ in the right-hand portion of Fig. 4, were observed only in the $\mathbf{E}\|\mathbf{B}$ spectra because adequate resolution is critical in this region of particularly closely-spaced absorption lines.[23]

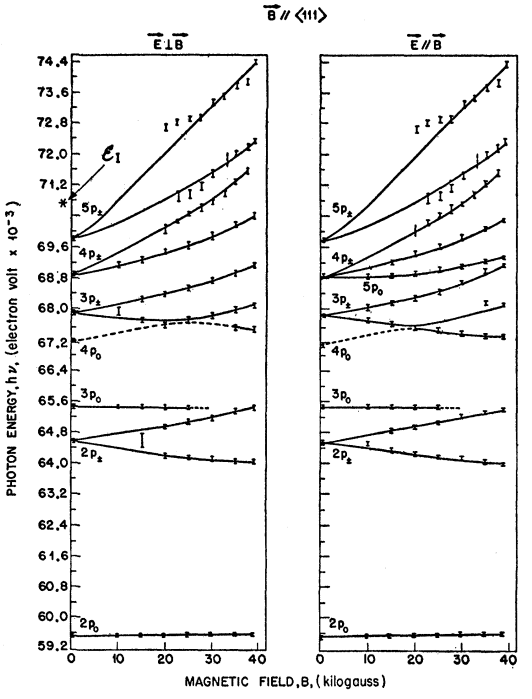

FIG. 4. Energy level diagram for fields up to 38.9 kgauss showing the energy of transitions from the Bi ground state in Si to the levels indicated. The small bars correspond to transmission minima such as those shown in Figs. 1 and 2 and their height indicates uncertainty in the position of the minimum.

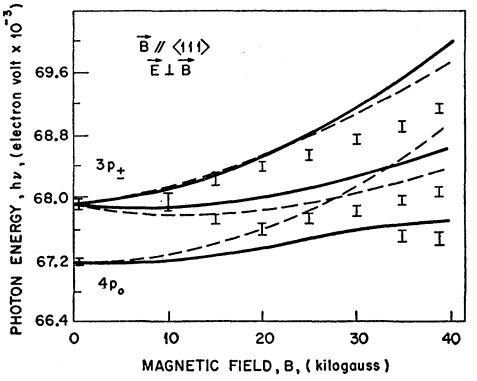

FIG. 5. Comparison of first-order perturbation theory (dashed curves) and second-order theory (solid curves) with experimental points for a typical set of levels. The interaction of the $4p_0$ with neighboring levels (second-order correction) is large and results in a reasonable fit to experimental points.

The curves through the experimental points of Fig. 4 illustrate the experimental behavior of each level as a function of magnetic field. A comparison of the shapes of these curves with the results of first-order perturbation theory gave good agreement for the lowest levels. However, first-order theoretical results do not fit the experimental curves for levels above $3p_0$. This disagreement made it necessary to extend the perturbation treatment to second order[16] to introduce the interactions among the various closely spaced Zeeman levels in this region. The correction to the first-order result consisted

[22] C. J. Rauch, J. J. Stickler, H. J. Zeiger, and G. S. Heller, Phys. Rev. Letters, 4, 64 (1960).

[23] It was always possible to use considerably narrower slit widths in the spectra with $\mathbf{E}\|\mathbf{B}$ in contrast to those with $\mathbf{E}\perp\mathbf{B}$ polarization because with the polarizer in the fore-optics a greater proportion of the source intensity is transmitted by the double pass prism monochromator for $\mathbf{E}\|\mathbf{B}$. Since $\mathbf{B}$ is horizontal and $\mathbf{E}$ vertical for the $\mathbf{E}\perp\mathbf{B}$ arrangement the reflection losses at the vertical prism faces are greater than for $\mathbf{E}\|\mathbf{B}$ as a consequence of the Brewster reflection effect.

principally of a sum of terms of the form

$$\frac{|\langle p_\pm|\mathcal{H}'|p_0\rangle|^2}{p_\pm - p_0} \tag{7}$$

where the energy denominator is the difference between first-order energies of the interacting levels. Figure 5 demonstrates the comparison between the experimental points and theoretical curves for the $4p_0$ and $3p_\pm$ levels computed for the case of $\mathbf{B}\|\langle 111\rangle$. The dotted curves of Fig. 5 are results of the first-order theory, showing the large deviation from the observed data. The second-order correction to the $4p_0$, greater than one millivolt at full field, produces better agreement as shown by the solid line. The strongest interactions among the p states were those which involved the p_0 levels. These interactions of the p_0 levels with many neighboring levels explains the apparent absence of the anticipated strong quadratic Zeeman effect for these levels with large quantum number. Furthermore, the smaller interaction of the $p_\pm$ levels explains why the marked influence of the high-field quadratic shift appears in the experimental data.

The anisotropy of the Zeeman effect of donor excited states in silicon was studied by making similar measurements with the magnetic field oriented parallel to each of the other two principal crystallographic directions.[24] The energy level diagram for $\mathbf{B}\|\langle 110\rangle$ is shown in Fig. 6. The splitting of the $1s \rightarrow 2p_\pm$ transition for $\mathbf{E}\perp\mathbf{B}$, as shown on the left-hand side of the figure, is larger than the $2p_\pm$ splitting for $\mathbf{B}\|\langle 111\rangle$. For $\mathbf{B}\|\langle 110\rangle$ in the crystal face and for propagation perpendicular to the $\{110\}$ face, the spectral contributions from various ellipsoids are no longer equivalent. The direction of the magnetic field makes an angle of 45° with the major axis of four of the conduction band ellipsoids and 90° with the other two. In Eq. (5), the factor $\cos\theta$ is now $1/\sqrt{2}$ for the first four ellipsoids, accounting for the larger splitting. The two ellipsoids at right angles to the field will not contribute to the splitting, and *might be* expected therefore, to contribute a "central" component to the Zeeman spectrum of the transition to the $2p_\pm$ level. The possibility of the occurrence of this central component in the Zeeman spectrum depends upon the transition selection rules involving the orientation of the electric vector relative to the major axes of the various ellipsoids, as given in Eq. (6). The absorption intensity contributed independently by each ellipsoid to the $1s \rightarrow 2p_\pm$ transition is proportional to $\sin^2\phi$ where ϕ is the angle between the electric vector and its major axis.

Two possible pairs of polarized Zeeman patterns can be observed for $\mathbf{B}\|\langle 110\rangle$ utilizing principal crystallographic planes and axes: (1) propagation perpendicular to a $\{100\}$ face with $\mathbf{B}\|\langle 110\rangle$ in the face and (2) propagation perpendicular to a $\{110\}$ face with $\mathbf{B}\|\langle 110\rangle$ in the face. In the first configuration, $\mathbf{E}$ will lie along a face diagonal for *both* polarization alignments and $\sin^2\phi$ will not vanish for any ellipsoid. Therefore, the central component would occur in the Zeeman spectrum for both polarization alignments and, indeed, both spectra of the pair would be identical. On the other hand, for the second configuration, although $\mathbf{E}$ is parallel to a face diagonal for $\mathbf{E}\|\mathbf{B}$, it is parallel to a *cube edge* for $\mathbf{E}\perp\mathbf{B}$. The two ellipsoids with their major axes parallel to *that* cube edge will not contribute to the $1s \rightarrow 2p_\pm$ absorption since, *for these alone*, $\sin^2\phi = 0$. The absence of the central component has the distinct advantage that one has only to resolve two instead of three absorption lines which would overlap at the lower fields. Figure 7 shows the $1s \rightarrow 2p_\pm$ absorptions for both polarization alignments where the intense central absorption for $\mathbf{E}\|\mathbf{B}$ prevents the resolution of the splitting except at the highest fields. Therefore, in order to resolve the splitting clearly, we chose arrangement (2), that is, propagation perpendicular to a $\{110\}$ face, for the anisotropy data presented in Fig. 6. This configuration is essential to observe the lower energy component of the $1s \rightarrow 3p_\pm$ transition in Fig. 6, where it was not resolved from the more intense central absorption in $\mathbf{E}\|\mathbf{B}$ but was clearly resolved in the $\mathbf{E}\perp\mathbf{B}$ spectrum. If, however, it had been necessary to study the weak absorptions above the $4p$ states (Fig. 4), arrangement (1) would have been used. The spectra for both polarizations would then be identical, the polarizer could be removed, and the weak transitions could be studied.

The simplest demonstration of the interaction of neighboring levels as they approach the same energy at high fields is shown on the left of Fig. 6, by the flattening of the curve for the higher energy component of

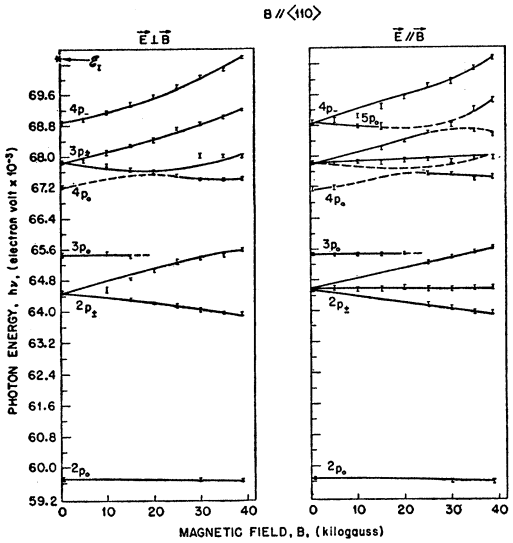

FIG. 6. Energy level diagram for Si(Bi) with the magnetic field along a ⟨110⟩ crystal direction.

[24] A complete tabulation of all spectral lines observed in both Si(Bi) and Si(Al) appears in Group Report M84-4 and may be obtained from The Hayden Library, Massachusetts Institute of Technology, Cambridge 38, Massachusetts. Hayden Reference H-24.

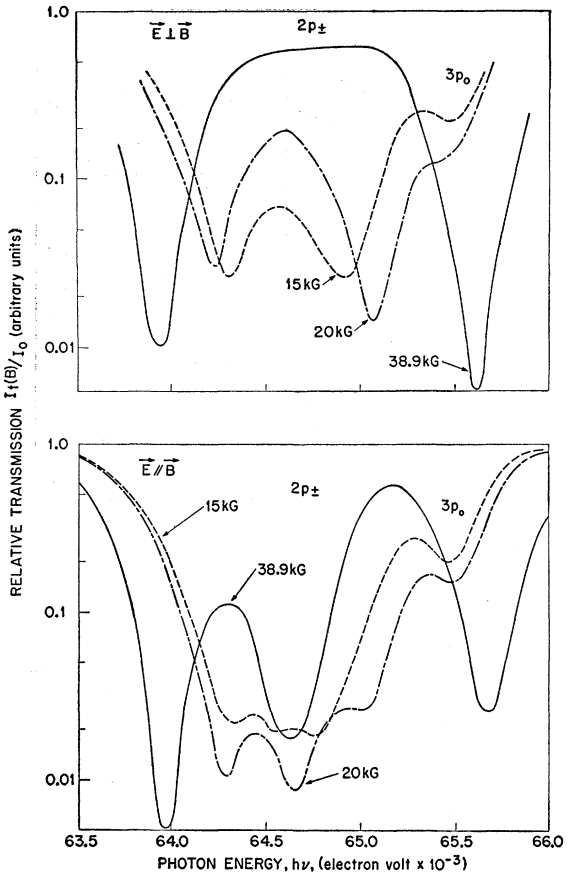

FIG. 7. The $1s \rightarrow 2p_{\pm}$ transition for the magnetic field along the $\langle 110 \rangle$ direction; (a) for the polarization $\mathbf{E} \perp \mathbf{B}$, the two absorption lines are well-resolved, (b) for $\mathbf{E} \| \mathbf{B}$, the central absorption line prevents resolution of the three lines at low fields.

the split $2p_{\pm}$ level. This effect was not seen in Fig. 4 because the splitting was smaller. The case for which the splitting is the maximum obtainable, namely, $\mathbf{B} \| \langle 100 \rangle$, is shown in Fig. 8. The curve for $2p_{\pm}$ on the left side shows that the interaction with the $3p_0$ is now so large above 25 kgauss that the linear splitting can no longer be used in Eq. (5) to evaluate the transverse electron effective mass as shown by the upper curves of Fig. 3.

The $\mathbf{E} \| \mathbf{B}$ spectrum of Fig. 8 has the unique property that no splitting can be observed for any level. Thus, in principle, one should be able to measure the quadratic Zeeman effect of all levels independently. However, it is clear that Fig. 8 does not show a quadratic effect which increases as n^4 because the second-order interactions between levels prevent the expected sharp increase in energy at high fields. The simplicity of the spectrum for $\mathbf{E} \| \mathbf{B}$ provided the opportunity to resolve any additional levels at high fields which could not possibly have been observed previously in the crowded region near the $4p_{\pm}$. This opportunity is enhanced by higher resolution available in the $\mathbf{E} \| \mathbf{B}$ polarization alignment as previously described.[23] An additional transmission minimum was indeed found lying between the $5p_0$ and $4p_{\pm}$ for both 38.9 kgauss and 30 kgauss. These minima may be related to a level lying very near to the $4p_{\pm}$ and $5p_0$ at zero field as indicated on the right-hand side of Fig. 8. Since splitting of levels cannot be observed in this spectrum, its identity could not be established experimentally.

B. Aluminum Acceptor

The spectrum of Fig. 9 shows the relative transmission through a six-millimeter specimen of aluminum-doped silicon for both zero field and the maximum field of 38.9 kgauss. The impurity concentration determined from Hall measurements was 2×10^{15} acceptors/cm^3. The levels have been numbered in order and each transition was identified by the notation of Hrostowski and Kaiser[12,25] (HK). The zero field energy of each absorption line agrees satisfactorily with the observations of HK with the exception of $1 \rightarrow 8$ which they did not report. This transition was rarely observable at zero field but could be traced from higher fields to a zero-field energy of 0.0680 electron volt. The transition marked $1 \rightarrow 9$ was observed by HK who called it $1 \rightarrow 8$.

The Zeeman spectrum of p-type silicon is much more complex than that shown by n-type. This is not unexpected in view of the complexity of the valence bands. For silicon the solution of a 6×6 matrix is required

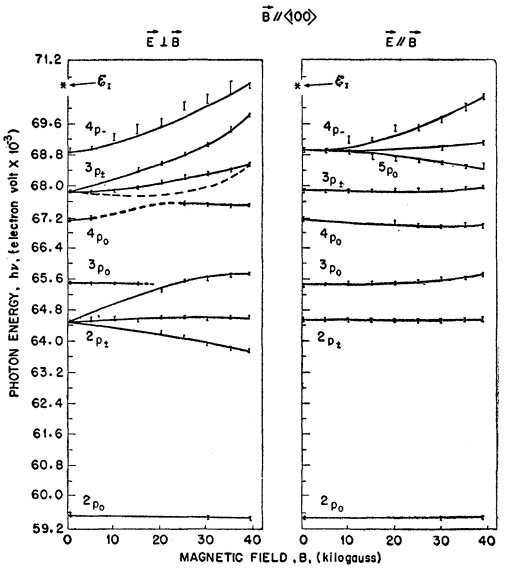

FIG. 8. Energy level diagram for Si(Bi) for the magnetic field along the $\langle 100 \rangle$ direction.

[25] The first five levels have been identified by Kohn[11] as $1s$, $2p^{(1)}$, $2p^{(2)}$, $2p^{(3)}$, and $2p^{(4)}$. However, since theory and experiment agree only for the first two excited states and theoretical values are lacking for the higher states, the HK nomenclature will be used here.

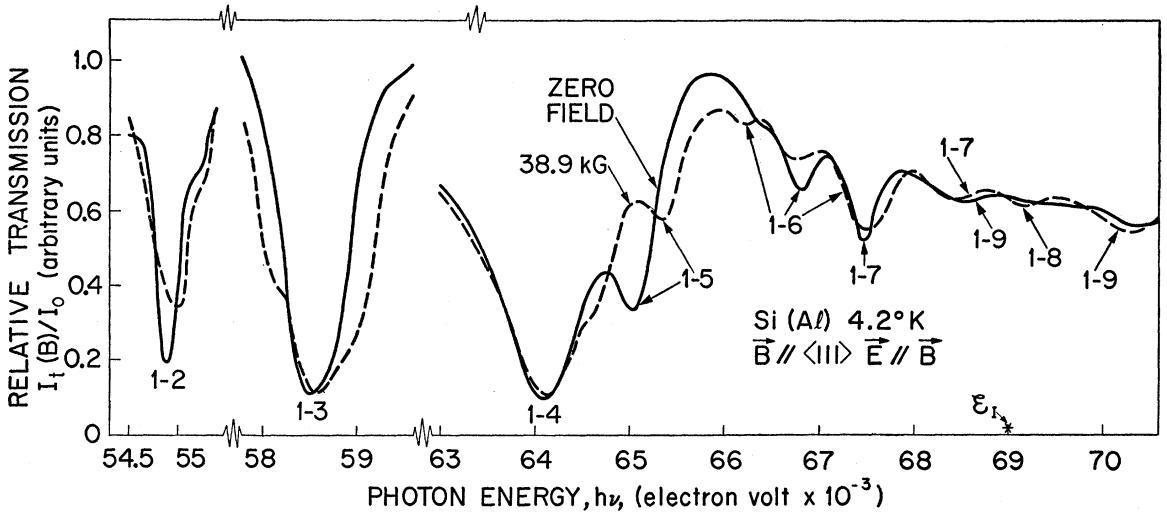

FIG. 9. Photoexcitation spectrum of the aluminum acceptor in silicon for zero field and 38.9 kgauss. The successive levels have been numbered in order.

because the spin-orbit split $p_{1/2}$ band ($\Delta=0.0441$ ev) [26] must be taken into account. This means that in solving the problem, even using two steps in the limit of infinite spin-orbit splitting, a 4×4 matrix must be solved and then the split-off band must be treated as a perturbation. Such a calculation has been carried out by Schechter[13] and the results indicate that the ground state, which is 4-fold degenerate, includes d-like states in addition to s-like states. Similarly, the first set of excited states which is normally associated with p-like functions also includes f-like functions. Altogether there are twelve states in this set which are grouped in order of their increased separation from the ground state into 4-fold, 4-fold, 2-fold, and 2-fold excited states. In addition to this, the s and p states of the split-off band are also coupled. Even if we neglect the contribution of the admixture of f and d states, the Zeeman pattern would be complex in view of the multiple degeneracy of each set. The maximum field available, 38.9 kgauss, is not sufficient to resolve completely such a structure in silicon. Consequently, it is not possible to give a thorough quantitative interpretation of the experimental observations which follow.

Unlike the Zeeman spectrum for the donor where the linear splitting was well resolved at 20 kgauss, the absorptions of Fig. 9 often showed no more than a substantial broadening even at maximum field. This feature is illustrated in the lower part of Fig. 10. It is characteristic of the $1\rightarrow2$ and $1\rightarrow3$ transitions to exhibit a broad absorption line at zero field which becomes progressively broader as the magnetic field is increased. In the lower part of Fig. 10, three minima can be seen in each 38.9 kgauss curve but these have not split sufficiently to be resolved. An indication of four unresolved minima can be detected in the left center curve of both Fig. 10 and Fig. 11 for the $1\rightarrow3$ transition. Neglecting additional possible structure for the admixed states, this would be consistent with the 4-fold degeneracy of levels

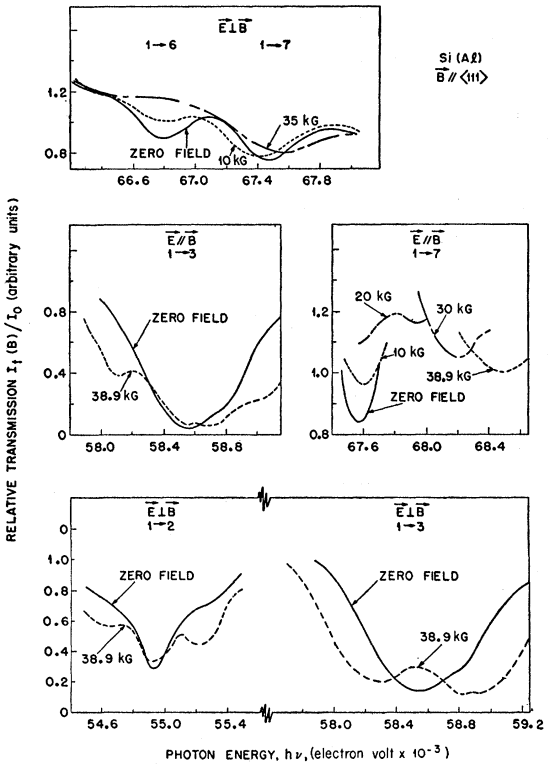

FIG. 10. Zeeman spectra of several transitions which illustrate the development of structure in the presence of a magnetic field. The structure is not yet resolvable at 38.9 kgauss in the $1\rightarrow2$ and $1\rightarrow3$ transitions. In the $1\rightarrow7$, a higher energy component grows stronger as the original line intensity decreases.

[26] S. Zwerdling, K. J. Button, B. Lax, and L. M. Roth, Phys. Rev. Letters 4, 173 (1960).

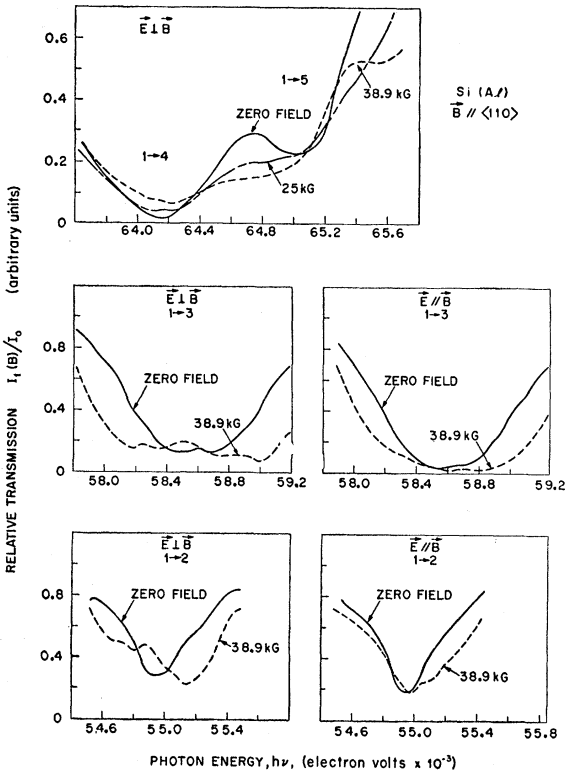

FIG. 11. Four extrema are detectable in the $1 \rightarrow 3$ transition for one polarization (left center) but not for the other (right center). Twofold degeneracy is indicated in the $1 \rightarrow 4$ and $1 \rightarrow 5$ transitions.

2 and 3. Although observations were made for both polarization alignments and for the magnetic field direction parallel to each of the three principal crystallographic axes, it was clear that in no case was the magnetic field intensity sufficiently large to split these four minima into resolvable absorption lines. The characteristics of the Zeeman spectra of the $1 \rightarrow 4$ and $1 \rightarrow 5$ transitions implied twofold degeneracy but again the structure was not resolvable. This twofold degeneracy is also consistent with the analysis of the levels. An example of the broadening and splitting of these absorptions is shown in the upper part of Fig. 11. For other orientations and polarizations, the structure was less definitive.

These first four transitions should correspond to those from the ground state to the first four excited states as designated by Kohn[11] in Table I. The agreement between theory and experiment at zero field is quite good for the $2p^{(1)}$ and $2p^{(2)}$ states, but not for the $2p^{(3)}$ and $2p^{(4)}$ states. No agreement was expected for the ground state of the aluminum acceptor since it is relatively deep and the effective mass approximation does not apply near the Coulomb center.

TABLE I. Zero-field ionization energies for the first four excited acceptor states in silicon. The theoretical values are those of Schechter[13] which are the same (within the fourth-place uncertainty quoted in parentheses) as those of Kohn.[11]

State	Energy (ev) Theory	Experiment
$2p^{(1)}$	0.0133 (7)	0.0136 (1)
$2p^{(2)}$	0.0094 (8)	0.0099 (1)
$2p^{(3)}$	0.0067 (3)	0.0044 (1)
$2p^{(4)}$	0.0044 (1)	0.0035 (1)

The Zeeman structure of the $1 \rightarrow 6$ and $1 \rightarrow 7$ transitions was usually well resolved and the $1 \rightarrow 6$ absorption line was observed to split into as many as three components while the $1 \rightarrow 7$ split into two for some orientations. A unique feature of these two transitions is best illustrated by the curves of the $1 \rightarrow 7$ transition shown in the right center of Fig. 10. As the field is increased, the primary absorption line becomes weaker and, at 20 kgauss a higher energy absorption line begins to develop. This line moves to higher energy with a linear dependence on magnetic field intensity while the original line decreases in intensity.

The transition energies observed for $\mathbf{B} \| \langle 110 \rangle$ are shown in Fig. 12. The data points shown represent the energy at which absorption maxima appeared in the spectra. It must be noted that this diagram cannot show the complete Zeeman pattern when the structure is not fully resolved. This is illustrated by the $1 \rightarrow 3$ transition which is shown in Fig. 12 to consist of four absorption lines for $\mathbf{E} \perp \mathbf{B}$ and only one for $\mathbf{E} \| \mathbf{B}$. Nevertheless, the center drawings of Fig. 11 show that the absorption line has broadened for both polarizations suggesting struc-

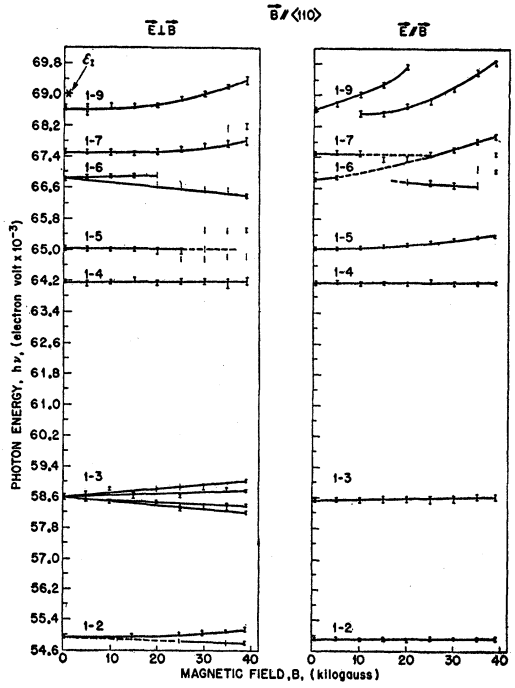

FIG. 12. Energy positions of detectable minima in the Zeeman spectrum of Si(Al) at 4.2°K. Structure is shown only for the lines that developed discrete minima. The broadening of a line and the onset of structure cannot be shown conveniently in this diagram.

ture, although this is indicated only for $\mathbf{E}\perp\mathbf{B}$. The same difficulty does not arise for the four uppermost levels which exhibit sharp, well-resolved absorption lines. Figure 13 shows the transition energies for $\mathbf{B}\|\langle 111\rangle$ in which the four uppermost levels were particularly well-defined for $\mathbf{E}\|\mathbf{B}$. There was a marked difference in the Zeeman spectra of these four levels for $\mathbf{E}\perp\mathbf{B}$, as shown in the figure. Additional differences in the behavior of these levels can be seen in the diagram for $\mathbf{B}\|\langle 100\rangle$ shown in Fig. 14. Some splitting appears for both polarizations for the $1\rightarrow 2$ and $1\rightarrow 3$ transitions and also for the $1\rightarrow 6$ and $1\rightarrow 7$ transitions indicating the multiple degeneracy of these states. These splittings appear essentially linear, with little or no quadratic behavior. This is consistent with the fact that the effective masses of the holes are approximately 0.2 m_0 and $0.5m_0$. However, there is a definite quadratic shift for the higher states which is most noticeable in the $1\rightarrow 9$ transition and is largest for $\mathbf{B}\|\langle 111\rangle$ with $\mathbf{E}\|\mathbf{B}$.

V. DISCUSSION

The object of performing Zeeman effect experiments on the excited states of impurities in semiconductors is chiefly to obtain quantitative information about the effective mass parameters of either the conduction or valence bands, to determine the nature of the energy surfaces involved and to find and identify the excited states of the impurity. The results obtained in this investigation of Si(Bi) have demonstrated that these objectives are achievable. The excited states have been identified up the fifth quantum level, the interpretation is completely consistent with the particular ellipsoidal nature of the conduction band in Si, and it has been possible to measure a value for the transverse effective mass of the electron of $(0.186\pm 0.006)m_0$. The method is uniquely capable of measuring much larger effective mass values in the infrared region than can be determined by either cyclotron resonance or magnetoabsorption in magnetic fields below 40 kgauss. In fact, the linear splittings observed in these experiments show that electron effective mass values as large as 0.5 m_0 could have been measured. A requirement for the resolution of the splitting of a simple line such as the $p_\pm$ levels in the donor spectrum is that $\omega_c\tau>1$. Thus, for an effective mass of 0.5 m_0 and $B=38.9$ kgauss, τ must be greater than 7×10^{-13} second. From the line width at half-power, τ was found to be greater than 10^{-12} second for the n-type silicon spectrum shown in Fig. 1. However, if the structure of the energy bands is very complex as for the valence bands in Si, the ability to measure effective mass values is severely limited by the multiplicity of spectral lines obtained. No attempt has been made to evaluate the hole effective mass from the Si(Al) data because of the multiple degeneracy of the levels and our subsequent inability to resolve the experimental spectral structure. The use of much larger magnetic field intensities than presently available would permit

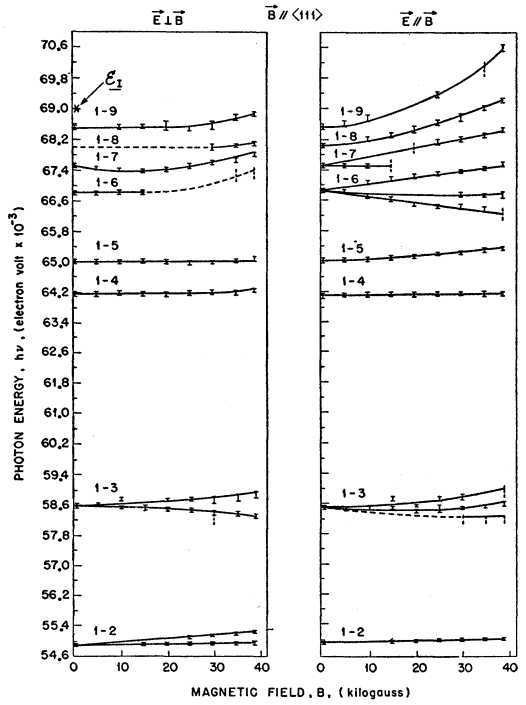

FIG. 13. The positions of minima for Si(Al) with $\mathbf{B}\|\langle 111\rangle$. Additional detail appears in the four highest levels for $\mathbf{E}\|\mathbf{B}$.

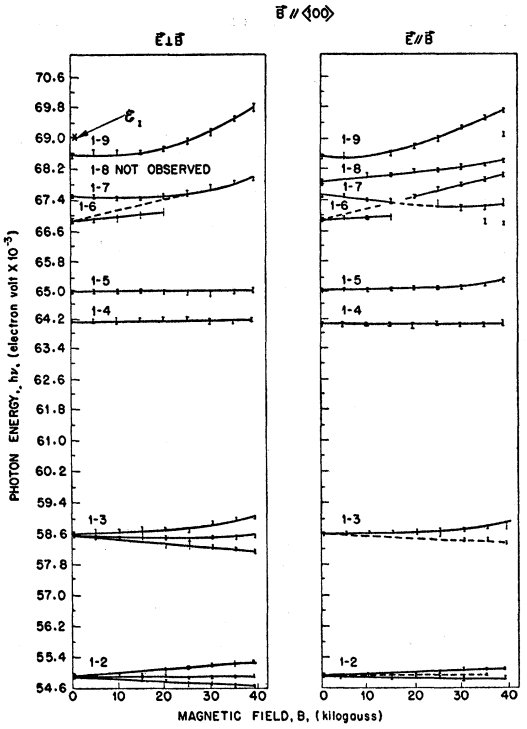

FIG. 14. The positions of minima for Si(Al) with $\mathbf{B}\|\langle 100\rangle$. The dotted bars indicate weak, unresolved shoulders in the spectrum.

the resolution of the structure and provide the basis for a theoretical evaluation of the effective mass of holes. The degeneracies that have been observed in the Si(Al) data appear to be consistent with present knowledge of the structure of the valence bands in Si.

In general, it is advantageous to select impurities which have the smallest ionization energies in order to enhance the probability of transitions from the ground state to the excited states as well as to the bound Landau levels in the continuum. This can be understood in terms of the overlapping of the wave functions for the states involved in the transition. The wave functions of the excited states are relatively independent of the depth of the ground state, but the ground-state wave function is strongly influenced by the Coulomb center. Experimentally, the absorption lines in the photoexcitation spectrum of shallow impurities will be relatively much more intense and their resolution will be improved. However, of the principal monovalent donors and acceptors in silicon, only the donor bismuth and the acceptor aluminum, which are not the shallowest, have excited states whose excitation spectrum occurs in the spectral region of maximum dispersion for a KBr prism. The choice of KBr prism dispersion combines the benefits of a spectral region for which a moderate source intensity is available and also one that is relatively free of atmospheric and silicon lattice absorptions. Furthermore, the benefits obtained in measuring spectra with the usual silver chloride sheet polarizer are limited to the region below 25 microns by the cutoff of that material. If one were to accept the experimental disadvantages of the longer wavelength region, then similar measurements of the shallower impurities, boron and antimony, would probably show the transitions to the bound Landau levels, which would reveal the effective mass of the carrier and the ionization energy of the impurity. Such results have been obtained in Ge for shallow impurities in the far infrared spectral region.[4,5,10]

It may be concluded from these observations of the Zeeman effect of excited impurity states in a semiconductor that the method provides a capability of making infrared measurements of heavy effective masses with the use of moderately high magnetic field intensities. Electron effective masses as large as m_0 could be measured with a field of 80 kgauss.

VI. ACKNOWLEDGMENTS

We are indebted to W. H. Kleiner and R. N. Brown for their helpful exchange of information during the course of this research and, in particular, for the use of some of their theoretical results prior to publication. We are grateful to J. P. Theriault for assistance with the experimental work, to E. P. Warekois for assistance with materials problems and, together with J. W. Sanchez, for x-ray orientation of the crystals. We wish to thank J. R. Williamson and Marion H. Andrews for their persistent efforts in the analysis of the data.

PHYSICAL REVIEW VOLUME 118, NUMBER 4 MAY 15, 1960

Rectification without Injection at Metal-to-Semiconductor Contacts

N. J. HARRICK
Philips Laboratories, Irvington-on-Hudson, New York
(Received December 7, 1959)

A recent publication shows that extraction in the semiconductor bulk may occur for either direction of current flow through the same metal-to-semiconductor contact when an insulating layer separates the metal and the semiconductor and the field effect determines the surface barrier under the metal. It is shown here that strong rectification, whose direction depends only on the bulk type, may occur for such contacts to extrinsic, but not intrinsic, semiconductors. Thus, rectification, without injection, may occur at the metal-to-semiconductor contact for the two-carrier system.

EXTRACTION in the semiconductor bulk can occur for either direction of current flow through the same metal-to-semiconductor contact if the field effect determines the surface barrier under the metal.[1,2] The field effect can predominate in this way when an oxide or other high resistance layer separates the metal and the semiconductor surface. It is the purpose of this paper to point out that strong rectification without injection[3] may occur for such contacts to extrinsic, but not intrinsic, semiconductors. This point and its implications for other semiconductors was not appreciated in an earlier discussion of this extraction phenomenon.[1]

Evidence for this phenomenon is shown in Fig. 1, which gives the J-V and J-Δp characteristics for two such metal-to-semiconductor contacts. Here the p-type bulk exhibited surface layers which were initially p^+, although similar curves were observed for this sample with n-type and neutral surfaces. Extraction is observed for negative currents (metal negative) with no saturation in the J-V characteristic. This is expected as the

[1] N. J. Harrick, Phys. Rev. **115**, 876 (1959).
[2] N. J. Harrick, Phys. Rev. Letters **2**, 199 (1959).
[3] The rectification mechanism described here is to be distinguished from the earlier rectification theories (i.e., diode and diffusion) which considered a one-carrier model and did not involve injection or extraction.